arXiv:0911.1143v3 [cond-mat.mes-hall] 8 Apr 2010

Variational Approach for the Effects of Periodic Modulations on the Spectrum of Massless Dirac Fermions

B. S. Kandemir and A. Mogulkoc
Department of Physics, Faculty of Sciences,
Ankara University, 06100
Tandoğan, Ankara, Turkey
(Dated: April 9, 2010)

In the variational framework, we study the electronic energy spectrum of massless Dirac fermions of graphene subjected to one-dimensional oscillating magnetic and electrostatic fields centered around a constant uniform static magnetic field. We analyze the influence of the lateral periodic modulations in one direction, created by these oscillating electric and magnetic fields, on Dirac like Landau levels depending on amplitudes and periods of the field modulations. We compare our theoretical results with those found within the framework of non-degenerate perturbation theory. We found that the technique presented here yields energies lower than that obtained by the perturbation calculation, and thus gives more stable solutions for the electronic spectrum of massless Dirac fermion subjected to a magnetic field perpendicular to graphene layer under the influence of additional periodic potentials.

PACS numbers: 73.61.Wp,73.20.-r,72.80.Rj

Since the discovery of graphene by Novoselov et. al[1], there have appeared many theoretical studies on graphene and graphene based nanostructures such as graphene quantum dots and graphene nanoribbons. There are also few reviews which have been devoted to these structures[2,3]. In most of these works, theoretical studies on the electronic energy spectrum of these structures have focused, due to their linear dispersion relation near K points in the Brillouin zone[4], on the continuum version of tight binding Hamiltonian, i.e., $2+1$ Dirac-Weyl equation[5], which has been confirmed by the experiments.[6]

The theoretical considerations of Weiss oscillations in an electrically modulated graphene were discussed by Peeters and Matulis[7]. They showed that, within the framework of non-degenerate first order perturbation theory , these non-relativistic oscillations are more pronounced in graphene as compared with those found for its $2D$ non-relativistic counterpart[8]. Very recently, studies on these oscillations in a magnetically modulated graphene have also been reported[9–13].

On the one hand, from the non-relativistic point of view, after Weiss et al.[14], theoretical studies on magnetoresistance oscillations in two-dimensional electron gas structures subjected to a periodic potential have been intensively studied for a long time within the frame work of perturbation theory[15]. It is shown that these oscillations have as a common origin the oscillating bandwidth of the modulation-broadened Landau bands[16]. On the other hand, role of one-dimensional periodic potentials is crucial itself in graphene. Very recently, it was shown that, by a Muffin-Tin type[17] one-dimensional periodic potential, velocity of charge carriers can be controlled in graphene. These type potentials allow one to create various types of graphene superlattices and to control the flow of charge carriers in an non-invasive way.

In this paper, we present a variational analysis of the combined effects of electric and magnetic potentials on the electronic energy spectrum of a Dirac-Weyl like electron in graphene. Our method is based upon the use of solutions of massless Dirac fermions in an uniform magnetic field as trial wave functions in the presence of external potentials. Analytical results obtained in this paper indicate that the variational method is more efficient than the other previously used methods, i.e., non-degenerate first-order perturbation theory.

The time independent effective massless Dirac-Weyl Hamiltonian we consider is $H = H_0 + U(\mathbf{r}_\perp)$, where

$$H_0 = v_F\ \boldsymbol{\alpha}\cdot\left[\mathbf{p}(\mathbf{r}) + \frac{e}{c}\mathbf{A}(\mathbf{r})\right]\ ,\ \boldsymbol{\alpha} = \begin{pmatrix}\boldsymbol{\sigma} & 0\\ 0 & -\boldsymbol{\sigma}\end{pmatrix} \tag{1}$$

is the Hamiltonian for an electron which is minimally coupled to magnetic field $\mathbf{B} = (0,0,B + B_0\cos Kx)$ with $K = 2\pi/a_0$, through the vector potential $\mathbf{A} = (0, Bx + (B_0/K)\sin Kx, 0)$. Here, $U(\mathbf{r}_\perp)$ is the one dimensional periodic electrostatic potential, and is given by $U(\mathbf{r}_\perp) = U\cos(K'x)$ with $K' = 2\pi/c'$.Here, a_0 and c' are the periods of magnetic and electrostatic modulations, respectively. In Eq.(1), we have used the Dirac-Pauli representation of Dirac matrix $\boldsymbol{\alpha}$ which is written of two by two-block form in terms of Pauli spin matrices $\boldsymbol{\sigma}$. Using two component spinor (pseudospin) as $\boldsymbol{\Psi}^\dagger = \begin{pmatrix}\phi^* & \chi^*\end{pmatrix}$ we see that each component of eigenvalue equation $H_0\Psi = E\Psi$ satisfies the following coupled first order differential equations:

$$\begin{aligned}\left(\boldsymbol{\sigma}\cdot\mathbf{p}+\frac{e}{c}\boldsymbol{\sigma}\cdot\mathbf{A}\right)\chi-\left[\widetilde{E}+U\left(\mathbf{r}_{\perp}\right)\right]\phi &= 0\\ \left(\boldsymbol{\sigma}\cdot\mathbf{p}+\frac{e}{c}\boldsymbol{\sigma}\cdot\mathbf{A}\right)\phi-\left[\widetilde{E}+U\left(\mathbf{r}_{\perp}\right)\right]\chi &= 0,\end{aligned} \tag{2}$$

where $\widetilde{E}=E/v_F$. Decoupling them in the absence of external potentials, Eq. (2) yields the second-order differential equation

$$H_0^{'}\phi\left(\mathbf{r}\right)=\left\{\left[p_x^2+\left(p_y+\frac{eB}{c}x\right)^2\right]+\frac{e\hbar B}{c}\sigma_3-\widetilde{E}^2\right\}\phi\left(\mathbf{r}\right), \tag{3}$$

where $\boldsymbol{\sigma}_3$ is the third component of the Pauli matrices. Since $\left[H_0^{'},p_y\right]=0$, we set

$$\phi\left(\mathbf{r}\right)=\frac{1}{\sqrt{L_y}}\exp\left(ik_y y\right)\phi(x). \tag{4}$$

Therefore, Eq. (3) reduces to the solution of second order equation for two-component wave function $\phi\left(x\right)$

$$\left\{\frac{d^2}{dx^2}-\left(k_y+\frac{eB}{\hbar c}x\right)^2+\left[\left(\frac{\widetilde{E}}{\hbar}\right)^2-\frac{eB}{\hbar c}\sigma_3\right]\right\}\phi\left(x\right)=0. \tag{5}$$

It is easy to show that, in pseudospin basis, the Hamiltonian $H_0^{'}$ in two-dimensions has solutions which can easily be expressed in terms of the Hermite polynomials by just setting with $\lambda=\left(\hbar c/eB\right)\left[\left(\widetilde{E}/\hbar\right)^2-\left(eBs/\hbar c\right)\right]=2\nu+1$. Therefore, the total solution of Eq. (2) can be written as

$$\Psi_{+}=\frac{\exp\left(ik_y y\right)}{\sqrt{L_y}}\begin{bmatrix}\mathbb{I}_{n-1}\left(\gamma\right)\\0\\0\\i\mathbb{I}_n\left(\gamma\right)\end{bmatrix},\Psi_{-}=\frac{\exp\left(ik_y y\right)}{\sqrt{L_y}}\begin{bmatrix}0\\\mathbb{I}_n\left(\gamma\right)\\-i\mathbb{I}_{n-1}\left(\gamma\right)\\0\end{bmatrix} \tag{6}$$

and with

$$\mathbb{I}_n\left(\gamma\right)=\left(\frac{\gamma^2}{\pi}\right)^{1/4}\frac{1}{\sqrt{2^n n!}}\exp\left\{-\gamma^2\left[x+x_0\right]^2/2\right\}H_n\left[\gamma\left(x+x_0\right)\right] \tag{7}$$

for the eigenvalues

$$\overline{E}_n^{(+)}=\sqrt{2neB/\hbar c} \tag{8}$$

which, in fact, corresponds to the eigenenergy $\overline{E}_n^{(+)}=\sqrt{2n}/\overline{\ell}$ for the π^* band of graphene, in which the quantum number n takes on the values $n=\nu+\left(s+1\right)/2$. One can follow the same procedure to obtain the associated two-component solutions of Eq. (1) for the hole part of spectrum, i.e., the π band of graphene corresponding to the eigenenergy $\overline{E}_n^{(-)}=-\sqrt{2n}/\overline{\ell}$. In Eqs. (5-7), we have defined $x_0=c\hbar k_y/eB$, and rescaled the energy $\widetilde{E}$ by dividing it by $\hbar$ to obtain $\overline{E}=\widetilde{E}\ /\hbar=E/\hbar v_F$, and defined $\gamma^2=eB/\hbar c$, $\overline{\ell}^2=\hbar c/eB$. Then, for the value $s=1$ we obtain $\nu=n-1$, and for $s=-1$ we obtain $\nu=n$. It should be noted that, $s=\pm1$ does not represent "spin up" and "spin down", but they describe states on the A(B) sublattice of graphene. In the presence of external potentials, to calculate their combined effects onto eigenvalues given by Eq. (8), we choose Eq. (6) and Eq. (7) as basis functions for our variational procedure. Therefore, in this sense one has to minimize the energy,

$$\overline{E}^{+}\left(\gamma\right)=\int d^2\mathbf{r}\Psi_{\pm}^{\dagger}\left(\gamma\right)\left[\boldsymbol{\alpha}\cdot\mathbf{p}+\frac{e}{\hbar c}\boldsymbol{\alpha}\cdot\left(0,Bx+\frac{B_0}{K}\sin Kx,0\right)+\overline{U}\left(\mathbf{r}_{\perp}\right)\right]\Psi_{\pm}\left(\gamma\right), \tag{9}$$

where $\overline{U}\left(\mathbf{r}_{\perp}\right)=U\left(\mathbf{r}_{\perp}\right)/\hbar v_F$. Analogously, one can follow the same treatment for the negative energy pseudospinors to obtain $\overline{E}^{-}\left(\gamma\right)$. Finally, performing the related integrals in Eq. (9), we find that

$$\begin{aligned}\overline{E}^{\pm}_{n\overline{k}_y}\left(\overline{\gamma}\right) &= \frac{\sqrt{2n}}{2}\overline{\gamma}+\frac{\sqrt{2n}}{2\cdot\overline{\ell}^{-2}\ \overline{\gamma}}+\frac{\sqrt{2n}}{2\pi^2\cdot\overline{\ell}_0^2}\overline{\gamma}\exp\left(-\pi^2/\overline{\gamma}^2\right)\cos\left(2\pi\overline{\ell}^2\overline{k}_y\right)\\ &\times\left[L_{n-1}\left(\frac{2\pi^2}{\overline{\gamma}^2}\right)-L_n\left(\frac{2\pi^2}{\overline{\gamma}^2}\right)\right]+\frac{\overline{U}}{2}\cdot\cos\left(2\pi p\overline{\ell}^2\overline{k}_y\right)\\ &\times\left[L_n\left(p^2\frac{2\pi^2}{\overline{\gamma}^2}\right)+L_{n-1}\left(p^2\frac{2\pi^2}{\overline{\gamma}^2}\right)\right]\exp\left(-p^2\pi^2/\overline{\gamma}^2\right)\end{aligned}\tag{10}$$

where the energy $\overline{E}^{\pm}_{n\overline{k}_y}\left(\overline{\gamma}\right)$ is again rewritten, for convenience, in the units of $\hbar v_F$, and all the lengths are in the units of a_0, $\overline{\gamma}=\gamma a_0$, $\overline{\ell}=\ell/a_0$, $\overline{\ell}_0=\ell_0/a_0$, $\overline{k}_y=k_y a_0$. Here, we have also defined $p=a_0/c'$. Therefore, our rescaled variables in Eq. (10) measure lengths in the units of a_0 and energies in the units of $\hbar v_F$. Eq. (10), when minimized with respect to $\overline{\gamma}$, gives the effect of external one dimensional electrostatic potential together with its magnetic analogue onto the Dirac-Weyl like Landau levels given by Eq. (8). To show this, we start from the well-known case, absence of external fields, i.e., B_0, U. In this case, minimization of Eq. (10) with respect to $\overline{\gamma}$ yields $\overline{\gamma}^2=eB/\hbar c=1/\overline{\ell}^2$. Replacing this result back into Eq. (10) yields

$$\begin{aligned}\overline{E}_{n\overline{k}_y}\left(\overline{\gamma}\right) &= \frac{\sqrt{2n}}{\overline{\ell}}+\frac{1}{2\pi^2}\sqrt{\frac{n}{2}}\frac{1}{\overline{\ell}_0^2\overline{\ell}}\exp\left(-\pi^2\overline{\ell}^2\right)\cos\left(2\pi\overline{\ell}^2\overline{k}_y\right)\\ &\times\left[L_{n-1}\left(2\pi^2\overline{\ell}^2\right)-L_n\left(2\pi^2\overline{\ell}^2\right)\right]+\frac{\overline{U}}{2}\cos\left(2\pi p\overline{\ell}^2\overline{k}_y\right)\\ &\times\left[L_n\left(2\pi^2p^2\overline{\ell}^2\right)+L_{n-1}\left(2\pi^2p^2\overline{\ell}^2\right)\right]\exp\left(-p^2\pi^2\overline{\ell}^2\right).\end{aligned}\tag{11}$$

It is easy to show that Eq. (11) reduces exactly to those found in Refs. [7,9] by using first-order perturbation correction. Of course, it covers inherently well-known Dirac like Landau levels, $\overline{E}^{+}=+\sqrt{2n}/\overline{\ell}$ in the absence of external fields. In FIG. 1(a), we plot dimensionless magnetic confinement length $\overline{\ell}$ variation of the dimensionless half bandwidth $\overline{E}_{n0}-\sqrt{2n}/\overline{\ell}$ for two different values of $U=0.5$ and 1 resulting from the numerical minimization of Eq. (10) (solid lines), together with the results of non-degenerate first-order perturbation calculation (dashed lines) as well as their difference $\Delta\overline{E}$ (lower panel). In order to observe the effect of one dimensional magnetic analogue in FIG. 1(b) we also plot the same in FIG. 1(a) but for $\chi=1$ ($\chi=B_0/U$) with $p=0.5$, 1, and 2, respectively. From both figures, as we decrease $\overline{\ell}$,i.e, increase $\overline{B}=B/\widetilde{B}$ ($\widetilde{B}=\hbar c/ea_0^2$) Landau levels broaden into mini subbands whose boundaries are determined by two asymptotic values of $\overline{k}_y$, i.e, by $\overline{k}_y=0$ and $\overline{k}_y=1/2\pi\overline{\ell}$. Of these only with $n=1$ and $n=2$ are depicted in FIG. 1(a) for $\overline{k}_y=0$.

It is clear from FIG. 1(a) and (b) that, as $\overline{\ell}$ decreases, dimensionless half bandwidth of the first two Landau levels begins to highly oscillate, due to the oscillatory nature of Laguerre polynomials, passing through degeneracy restoring points, i.e., wherein the flatband condition is fulfilled, and thus Weiss oscillations are suppressed. It should also be noted that, from the lower panels, a rapid increase of $\Delta\overline{E}$ with increase in U is evident, yielding significant discrepancies above $0.1\hbar v_F$. Moreover, note that $\Delta\overline{E}$ diminishes at some values of $\overline{\ell}$ where approximately flatband condition is fulfilled. In other words, since diminishing $\Delta\overline{E}$ indicates that the variational and the perturbational results are almost same, we can say that, around these points, i.e., where the flatband condition is fulfilled, perturbational results can be safely used, but otherwise they cannot.

We further plot in FIG 2 the variations of dimensionless variational parameter $\overline{\gamma}$ as a function of dimensionless magnetic confinement length $\overline{\ell}$ for the first two Landau levels with different p values. Also, for comparison, the curve for the unperturbed case, i.e., $\overline{\gamma}=1/\overline{\ell}$, is plotted (dashed bold line). We note two features of these curves. First, there exist discrepancies between the unperturbed and perturbed curves in the high magnetic field regime, $\overline{\ell}<1$ where the variational picture becomes more appropriate. Second, again in this region the perturbed curves intersect the unperturbed one wherein the flatband condition is fulfilled, as is indicated above. These justify the validity of our variational procedure.

In FIG. 3, $\overline{E}_{n0}$ as a function of $\sqrt{\overline{B}}$ are plotted for the first four Landau levels. With increasing $\overline{B}$ strong deviations from the unperturbed Dirac-Weyl like Landau levels (dashed ones) appear near $\overline{B}\sim 1$. To see these effects more clearly, variations of half-bandwidths of the corresponding levels, i.e., $\Delta\overline{E}_{n0}=\overline{E}_{n0}-\sqrt{2n\overline{B}}$, are given as a function of $\sqrt{\overline{B}}$ in the lower panel of the same figure.

Finally, in FIG. 4(a) and (b) we have plotted $\overline{E}_{n0}$ as a function of $\sqrt{\overline{B}}$ for the four p values, and for the four χ values, respectively. It should be noted that the variable $p = a_0/c'$ measure whether oscillating fields are in phase or out of phase, and the variable χ measures the ratio of amplitudes of fields. One observes very clearly that, by changing their phases and/or their ratios of amplitudes, dramatic changes in the spectrum occur when $\overline{B}$ decreases.

In conclusion, since our variational method yields energies lower than that obtained by the first-order perturbation calculation, it provides an efficient procedure for finding out the effects of external potentials onto the electronic spectrum of a graphene electron in an uniform magnetic field. Moreover, we see that, after performing various analytical checks on the obtained energy spectra, our results cover the well-known results found in the literature[7,9], and in the absence of external fields they reduce to the $2D$-Landau levels of massless Dirac fermions in some certain values of variational parameter. We use the solutions of massless Dirac fermions in an uniform magnetic field as trial wave functions to obtain the low-lying energy spectrum of these particles in the presence of external potentials. For Landau bands with high indices in the case of high magnetic fields, adjacent Landau bands may overlap. In this case, the variational function should be a linear combination of these sates rather than one of them. In this regime, as a consequence of overlapping, even-odd transitions in the Shubnikov-de Haas oscillations[18] may be expected in the graphene.

Acknowledgments

The authors thank Professor T. Altanhan for valuable discussions, and for a critically reading of the manuscript.

[1] K. S. Novoselov, A. K. Geim, S. V. Morozov, D. Jiang, Y. Zhang, S. V. Dubonos, I. V. Grigorieva, and A. A. Firsov, Science **306**, 666 (2004).
[2] A. H. Castro Neto, F. Guinea, N. M. R. Peres, K. S. Novoselov, and A. K. Geim, Rev. Mod. Phys. **81**, 109 (2009).
[3] Eduardo V. Castro, K. S. Novoselov, S. V. Morozov, N. M. R. Peres, J. M. B. Lopes dos Santos, Johan Nilsson, F. Guinea, A. K. Geim, and A. H. Castro Neto, arXiv:0807.3348v1 [cond-mat.mes-hall] (2008).
[4] P. R. Wallace, Phys. Rev. **71,** 622 **(**1947**)**.
[5] Gordon W. Semenoff, Phys. Rev. Lett. **53**, 2449 (1984).
[6] K. S. Novoselov, A. K. Geim, S. V. Morozov, D. Jiang, M. I. Katsnelson, I. V. Grigorieva, S. V. Dubonos, and A. A. Firsov, Nature **438**, 157 (2005); Yuanbo Zhang, Yan-Wen Tan, Horst L. Stormer, and Philip Kim, Nature **438**, 201 (2005); Taisuke Ohta, Aaron Bostwick, J. L. McChesney, Thomas Seyller, Karsten Horn, and Eli Rotenberg, Phys.Rev.Lett. **98**, 206802 (2007) .
[7] A. Matulis and F. M. Peeters, Phys. Rev. B. **75**, 125429 (2007).
[8] F. M. Peeters and P. Vasilopoulos , Phys. Rev. B. **47**, 1466 (1992).
[9] J. Milton Pereira, F.M. Peeters, and P. Vasilopoulos, Phys. Rev. B. **75** , 125433 (2007); M. Tahir and K. Sabeeh, J. Phys.: Condens. Matter **19**, 406226 (2007); M. Tahir and K. Sabeeh, Phys. Rev. B. **76**, 195416 (2007); M. Tahir and K. Sabeeh, Phys. Rev. B. **77**, 195421 (2008).
[10] M. Ramezani Masir, P. Vasilopoulos, and F.M. Peeters, New J. Phys. **11**, 095009 (2009); M. Ramezani Masir, A. Matulis, and F.M. Peeters,Phys. Rev. B **79**, 155451 (2009);M. Ramezani Masir, P. Vasilopoulos, and F.M. Peeters, Phys. Rev. B **79**, 035409 (2009); M. Ramezani Masir, P. Vasilopoulos, and F.M. Peeters, Appl. Phys. Lett. **93**, 242103 (2008); M. Ramezani Masir, P. Vasilopoulos, A. Matulis, and F.M. Peeters, Phys. Rev. B **77**, 235443 (2008).
[11] Quan-Sheng Wu, Sheng-Nan Zhang, and Shie-Jie Yang, J. Phys.: Condens. Matter **20**, 485210 (2008); M. Barbier, F.M. Peeters, P. Vasilopoulos, and J. Milton Pereira, Phys. Rev. B **77**, 115446 (2008); *ibid*, Phys. Rev. B **80**, 205415 (E) (2009).
[12] Y. H. Chiu, J. H. Ho, C. P. Chang, D. S. Chuu, and M. F. Lin, Phys. Rev. B. **78,** 245411 (2008).
[13] Luca Dell'Anna and Alessandro De Martino, Phys. Rev. B. **79,** 045420 (2009).
[14] D. Weiss, K. V. Klitzing, K. Ploog, and G. Weimann, Europhys. Lett., **8**, 179 (1989).
[15] R. R. Gerhardts, D. Weiss, and K.v. Klitzing, Phys. Rev. Lett. **62**, 1173 (1989); Mayumi Kato, Akira Endo, Shingo Katsumoto, and Yasuhiro Iye, Phys. Rev. B **58**, 4876 (1998).
[16] Chao Zhang and Rolf R. Gerhardts, Phys. Rev. B **41**, 12 850 (1990).
[17] Cheol-Hwan Park, Li Yang, Young-Woo Son, Marvin L. Cohen, and Steven G. Louie, Nature Phys. **4**, 213 (2008); *ibid*, Phys.Rev.Lett. **101**, 126804 (2008).
[18] Jirong Shi, F. M. Peeters, K. W. Edmonds and B. L. Gallagher, Phys. Rev. B. **66**, 035328 (2002).

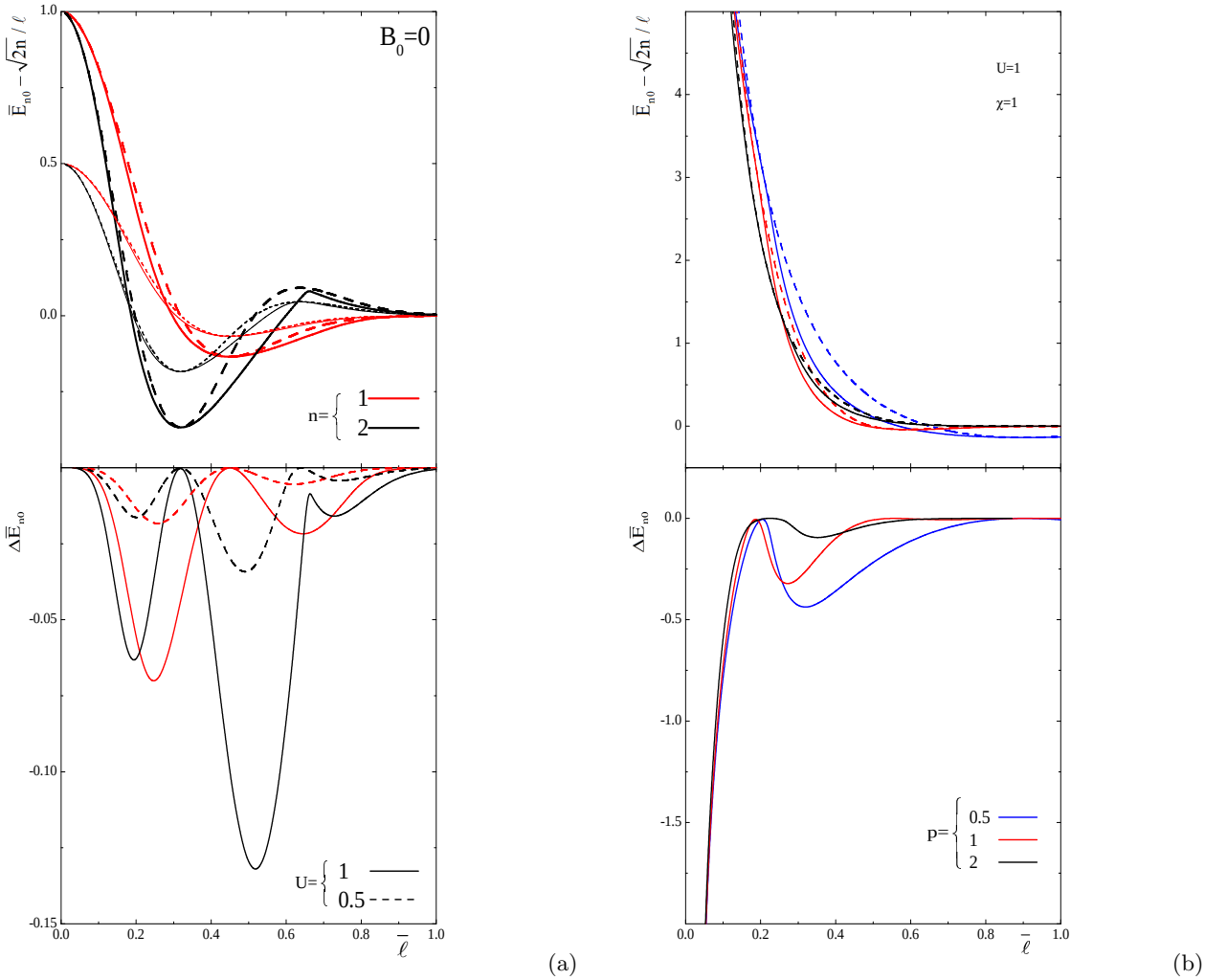

FIG. 1: (a) $\overline{E}_{no} - \sqrt{2n}/\overline{\ell}$ as a function of dimensionless magnetic confinement length $\overline{\ell} = \ell/a_0$ for the first two Landau levels, i.e. for $n = 1, 2$, in the absence of magnetic modulation for $U = 1$ and $U = 0.5$ with $\overline{k}_y = 0$. While the solid curves represent the present theoretical calculations, the dashed ones corresponds calculations using first order non-degenerate perturbation theory presented in Ref. 7. In upper panel, while upper curves represent the $U = 1$, lower curves corresponds to the $U = 0.5$. (b) The same as in (a), but for $U = 1$ and $\chi = 1$. In both figures, the two theoretical curves are compared with each other by plotting their difference $\Delta\overline{E}_{n0} = \overline{E}^{V}_{n\overline{k}_y} - \overline{E}^{PT}_{n\overline{k}_y}$ as a function of dimensionless magnetic confinement length $\overline{\ell}$ where $\overline{E}^{V}_{n\overline{k}_y}$ and $\overline{E}^{PT}_{n\overline{k}_y}$ denote the results of present work and non-degenerate perturbation theory, respectively (lower panels).

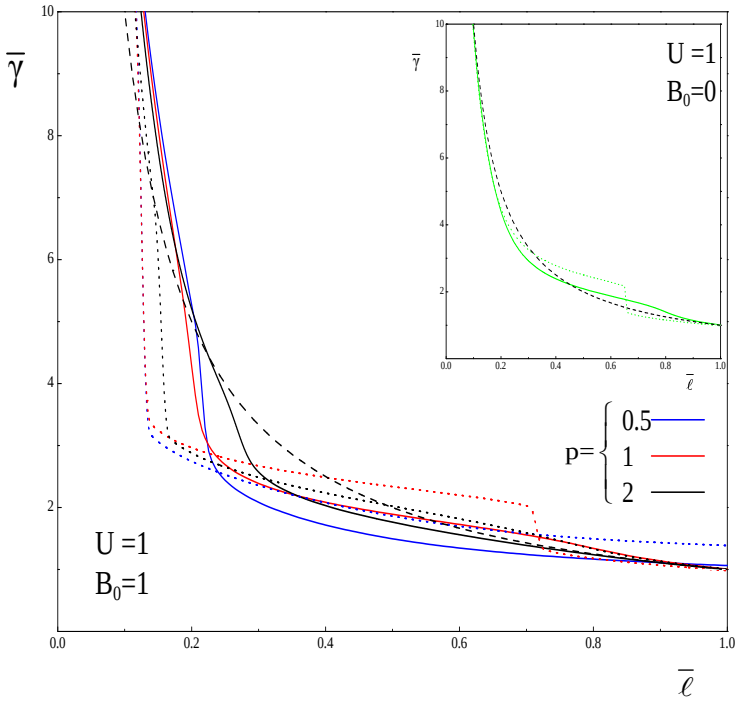

FIG. 2: The dimensionless variational parameter $\overline{\gamma}$ as a function of dimensionless magnetic confinement length $\overline{\ell}$. While the solid lines correspond to energy level with $n = 1$, the dotted lines correspond to energy level with $n = 2$, for various sets of p. The inset shows the $B_0 = 0$ case for $U = 1$.

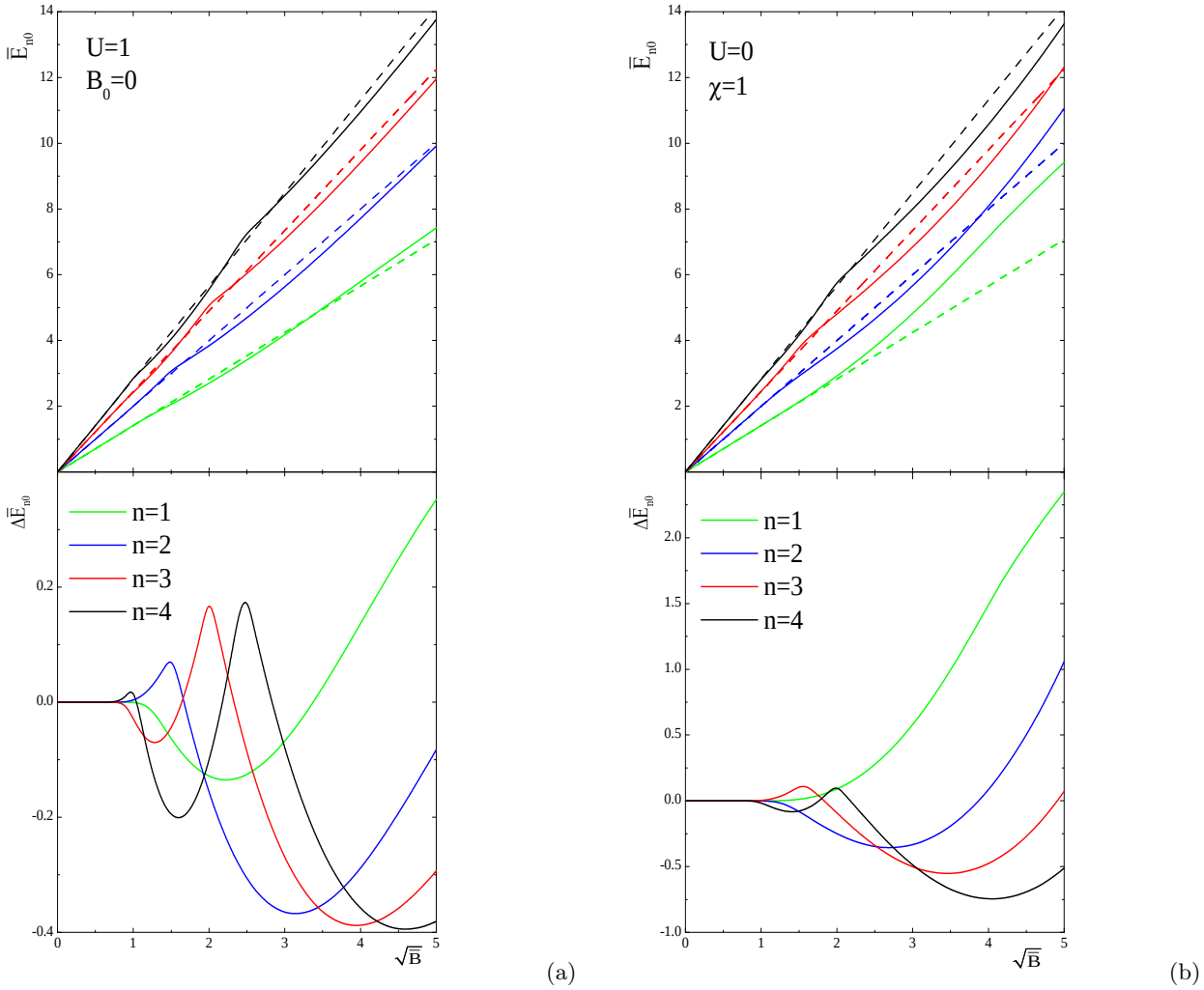

(a) (b)

FIG. 3: (a) The first four low-lying Landau levels as a function of $\sqrt{\overline{B}}$ with $U = 1$ for $B_0 = 0$, and for $\overline{k}_y = 0$. While the dashed curves correspond to unperturbed Landau levels, i.e.,$\sqrt{2n\overline{B}}$, the solid ones denotes the effect of electrostatic potential, (upper panel). To demonstrate the effect of external modulated electrostatic potential $\overline{E}_{n0} - \sqrt{2n\overline{B}}$ is also plotted as a function of $\sqrt{\overline{B}}$, in lower Panel. (b) The same as in (a), but for $U = 0$ and $\chi = 1$.

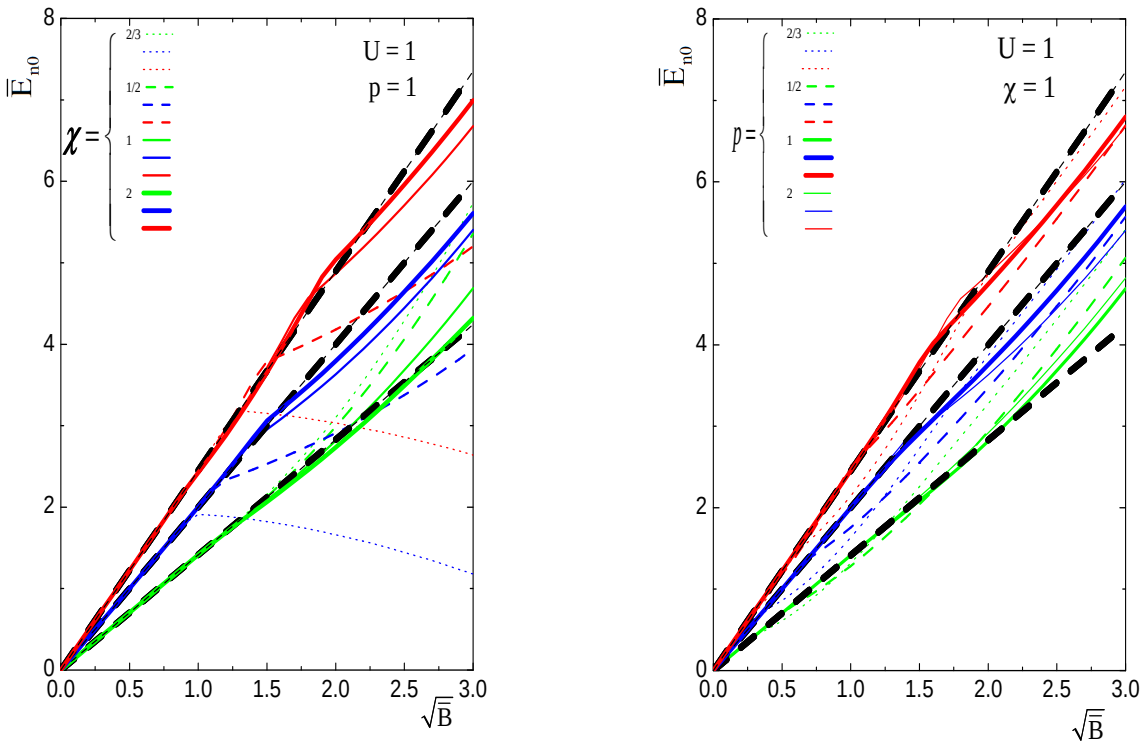

(a) (b)

FIG. 4: The same as in FIG. 2, but for various sets of p and χ, and only for the first three energy levels. The bold dashed straight lines refer to the relevant unperturbed Landau levels